






Activation of Microwave Signals in Nanoscale Magnetic Tunnel Junctions by Neuronal Action Potentials

Jose Miguel Algarin¹ , Bharath Ramaswamy², Lucy Venuti^{3,4}, Matthews E. Swierzbinski^{3,4}, James Baker-McKee⁷, Irving N. Weinberg⁷ , Yu-Jin Chen⁸, Ilya N. Krivorotov⁸ , Jordan A. Katine⁹, Jens Herberholz^{3,4}, Ricardo C. Araneda^{4,5} , Benjamin Shapiro^{2,6}, and Edo Waks¹ 

¹ Institute for Research in Electronics and Applied Physics, University of Maryland, College Park, MD 20742, USA

² Fischell Department of Bioengineering, University of Maryland, College Park, MD 20742, USA

³ Department of Psychology, University of Maryland, College Park, MD 20742, USA

⁴ Neuroscience and Cognitive Science Program, University of Maryland, College Park, MD 20742, USA

⁵ Department of Biology, University of Maryland, College Park, MD 20742, USA

⁶ Institute for Systems Research, University of Maryland, College Park, MD 20742, USA

⁷ Weinberg Medical Physics, Inc., North Bethesda, MD 20852, USA

⁸ Department of Physics and Astronomy, University of California, Irvine, CA 92697, USA

⁹ HGST Research Center, San Jose, CA 95135, USA

Received 3 Nov 2018, revised 29 Nov 2018, accepted 11 Dec 2018, published 30 Jan 2019, current version 15 Feb 2019.

Abstract—Action potentials are the basic unit of information in the nervous system, and their reliable detection and decoding holds the key to understanding how the brain generates complex thought and behavior. Transduction of these signals into microwave signal oscillations can enable wireless sensors that report on brain activity through magnetic induction. In this letter, we demonstrate that action potentials from the lateral giant neurons of crayfish can induce microwave oscillations in nanoscale magnetic tunnel junctions (NMTJs). We show that action potentials activate microwave oscillations in NMTJs with an amplitude that follows the action potential signal, demonstrating that the device has both the sensitivity and temporal resolution to respond to action potentials from a single neuron. The activation of magnetic oscillations by action potentials, together with the small surface area and the high-frequency tunability, makes these devices potential candidates for high-resolution sensing of bioelectric signals from neural tissues. These device attributes may be useful for the design of high-throughput bidirectional brain–machine interfaces.

Index Terms—Biomagnetics, biosensors, magnetic nanoparticles, nanosensors, spintronics, neurons, action potentials, magnetic tunnel junctions, microwave oscillations.

I. INTRODUCTION

At its core, the brain is a complex network of neurons connected by synapses. Action potentials are the fundamental units of communication between neurons that form the basic building blocks for thought and behavior [Koch 2000, Gerstner 2002, Mareschal 2007]. Detecting these action potentials wirelessly with high spatial and temporal resolution is highly useful to understand how the brain processes information and thought [Koch 2000], as well as to diagnose and treat neurological diseases [Meisler 2005, Mantegazza 2010, Ben-Ari 2012].

A number of different techniques exist for wirelessly measuring human brain activity. For example, functional magnetic resonance imaging provides wireless measurements with spatial resolutions on the order of millimeters [Matthews 2006]. However, this technique only measures brain activity indirectly through hemodynamic effects. Furthermore, it does not have the spatial and temporal resolution to isolate single neurons or small clusters and read out individual action potentials [Belliveau 1992, Frahm 1993]. Other methods, such as magnetoencephalography, provide excellent temporal resolution in the

milliseconds range but exhibit very poor spatial resolution [Haemaelainen 1993]. Combining functional magnetic resonance imaging with electroencephalography or magnetoencephalography could potentially yield improved temporal resolution [Dale 1993], but spatial resolution still remains in the millimeters range. Currently, the most advanced method for performing highly localized measurements of neuronal action potentials in humans and other primates involves surgical implantation of electrodes to target areas of the brain [Rothschild 2010]. Seo [2016] demonstrated an ultrasonic backscatter system that enables communication with such implanted bioelectronics in the peripheral nervous system. Other techniques, such as optical methods based on voltage-sensitive contrast agents (dyes, quantum dots) and optogenetics have also been demonstrated [Millard 2004, Canepari 2010, Fenno 2011, Aston-Jones 2013]. But focused optical beams cannot penetrate the skull or deep tissue and, thus, cannot access deep brain regions [Abdo 2007]. Currently, there is great need in neuroscience for new methods to transduce biological activity to wireless signals that can penetrate through deep tissue.

The application of spintronics to biological sensing remains a relatively unexplored area that has potential to resolve some of the difficult challenges inherent to wireless signal detection. Recent work has incorporated giant magnetoresistors into electrode arrays to perform magnetoencephalography [Caruso 2017], but this technique

is not wireless. Another compelling spintronic device is the nanoscale magnetic tunnel junction (NMTJ), which takes as an input small direct currents and converts them to microwave oscillations [Kiselev 2003, Rippard 2004, Deac 2008, Houssameddine 2008, Zhou 2008, Torrejon 2017, Zhang 2018] that can report wirelessly to a receiver by electromagnetic coupling [Ramaswamy 2016]. The NMTJ is nanoscale in dimensions and can operate at microwave frequencies ranging from 0.1–10 GHz. This property presents a potential solution to the long-standing challenge inherent to oscillators based on electrical LC circuits that are difficult to scale down to small dimensions. A standard LC circuit of 10 μm dimensions typically exhibits oscillation frequencies exceeding 100 GHz, due to limits in achievable values of inductance and capacitance [Seo 2016]. But these frequencies are incompatible with biological tissues, which become highly absorbing above 5 GHz. The NMTJ can operate at biologically compatible frequencies while maintaining nanoscale dimensions. Furthermore, they can operate with small input currents, on the order of a microampere, which may be sufficiently low to be directly driven by neurons without the need for amplifiers. Finally, the oscillation frequency of the device shifts in the presence of an external magnetic field [Kiselev 2003, Slavin 2009], enabling the precession frequency to encode spatial information by applying a magnetic field gradient, analogous to conventional magnetic resonance imaging. These properties make NMTJs promising candidates for detecting weak bioelectric signals with high spatial precision, potentially, up to single-cell resolution. However, prior to wireless transduction of biological signals, the ability of NMTJs to transduce biological signals to microwave oscillations needs to be addressed.

Here, we demonstrate that an NMTJ can transduce a biological signal to microwave signals. We drive the device with action potentials from crayfish neurons. Crayfish possess giant neurons that generate voltages on the order of a few millivolts when measured with extracellular recording electrodes, making them an ideal system to study spintronic devices. We utilized the extracellular voltage produced by the lateral giant neuron to drive the device and observed a clear microwave signal whose temporal envelope accurately reproduced the action potential waveform. This result shows that spintronic devices could potentially serve as nanoscale sensors for bioelectric signals with high spatial resolution and sufficient bandwidth to temporally resolve neuronal action potentials.

The lateral giant escape circuit of crayfish is one of the best understood neuron circuits in the animal kingdom [Edwards 1999, Herberholz 2012]. The lateral giant neurons receive mechanosensory inputs in all abdominal segments and produce single action potentials that propagate along the entire ventral nerve cord, the caudal part of the crayfish nervous system, to activate flexor motor neurons [Wine 1983, Herberholz 2002]. In freely behaving animals, this leads to a rapid flexion of the tail and a stereotyped forward “tail-flip” that thrusts the animal away from an attacking predator [Herberholz 2004]. The lateral giants are the largest neurons in the ventral nerve cord with axon diameters of up to 200 μm in adult crayfish and can be readily stimulated with extracellular silver wire electrodes both in intact animals and in isolated nerve cords [Swierzbinski 2017]. The extracellular (field) potential generated by the lateral giant spike is large enough to be recorded outside the animals during a naturally evoked tail-flip [Herberholz 2001]. These large extracellular fields make the lateral giant neurons suitable biological models to be interfaced with NMTJs and produce a microwave signal.

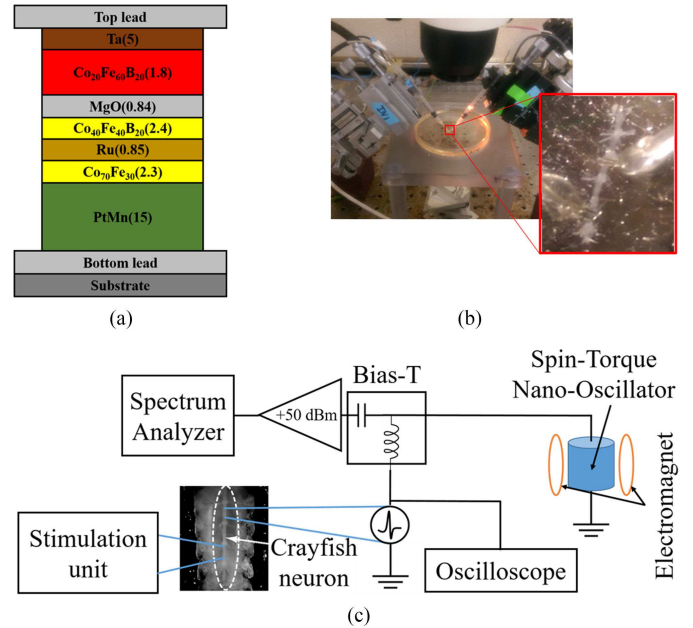


Fig. 1. (a) Schematic of the nanopillar magnetic tunnel junction device. The numbers in parentheses are the layer thicknesses in nanometers. (b) Picture of experimental setup used for crayfish neuron stimulation and recording. (c) Schematic of the circuit to trigger the NMTJ with action potentials from a crayfish neuron.

II. METHODS

The NMTJ that we employ is an elliptical magnetic tunnel junction nanopillar with lateral dimensions 50 nm \times 190 nm. Fig. 1(a) shows the complete layer structure for the device, with thicknesses (in nanometers) indicated in parentheses. We deposited all layers using magnetron sputtering in a Singulus TIMARIS system, and patterned the magnetic tunnel junctions using electron beam lithography followed by ion milling. The synthetic antiferromagnet is PtMn/ $\text{Co}_{70}\text{Fe}_{30}$ / $\text{Ru}/\text{Co}_{40}\text{Fe}_{40}\text{B}_{20}$ with the $\text{Co}_{70}\text{Fe}_{30}$ pinned layer and the $\text{Co}_{40}\text{Fe}_{40}\text{B}_{20}$ reference layer antiferromagnetically coupled by the tuned thickness of Ru. Prior to patterning, we anneal the multilayer for 2 h at 300 $^{\circ}\text{C}$ in a 1 T in-plane field to set the pinned layer exchange bias direction parallel to the long axis of the nanopillars. At equilibrium, all magnetic layers have magnetic moments lying in the plane of the sample. The resistance-area product for the MgO thickness depicted is approximately 4.5 $\Omega \cdot \mu\text{m}^2$.

We obtained adult crayfish (*Procambarus clarkii*) of both sexes from a commercial supplier and kept them in large communal tanks before the experiments. Individual animals (total body lengths 7–10 cm, measured from rostrum to telson) were anaesthetized on ice for several minutes until immobility. We separated the abdomen from the anterior part of the body and pinned it down in a petri dish. We removed the membrane covering the ventral nerve cord and muscles, cut all ganglionic nerves, and dissected out the ventral nerve cord. Next, we firmly pinned down the ventral nerve cord dorsal side up in a round petri dish lined with silicone elastomer (Sylgard) and filled with fresh crayfish saline [see Fig. 1(b)]. The saline in the dish maintained a constant temperature of 20 $^{\circ}\text{C}$ –21 $^{\circ}\text{C}$ throughout the experiments. Only preparations that appeared healthy were used, which allowed continuous measurements for several hours after the dissection.

We placed a pair of silver wire electrodes on the upper side surface of the ventral nerve cord to stimulate the lateral giant neuron

and a second identical pair of electrodes near the frontal end of the nerve cord to record the lateral giant action potential [see Fig. 1(b)]. To evoke lateral giant action potentials, we applied voltage pulses with amplitudes of 5–10 V and pulse durations of 0.2–0.5 ms to the ventral nerve cord. We stimulated using a data acquisition board (NI USB-6211) controlled by a LabVIEW (National Instruments, Austin, TX, USA) program. We used a differential amplifier (A-M Systems, Model 1700) for stimulations and recordings. A stimulus isolation unit (Grass, Model SIU5) applied a constant voltage stimulus. We used an amplifier with $1000\times$ of gain to amplify the recorded signals, and then measured the signal using an oscilloscope (Lecroy HRO 64Zi). The lateral giant action potential can be easily identified by its characteristic shape, large amplitude, fast conduction velocity, and low firing threshold. However, because we performed extracellular recordings, the shape of the recorded signal depends on factors, such as electrode position and orientation, and this will vary from experiment to experiment. This variability was more prominent when using the NMTJ because it required using one recording electrode as a ground electrode; among some other minor effects, this substantially reduced the amplitude of the recorded action potential. We stimulated the crayfish neuron at subthreshold level as controls to confirm that recording experiments evoked neural activity. Since thousands of stimuli at high frequency can lead to occasional failure in the lateral giant neurons, we obtained best results with longer interstimulus intervals. In total, we were able to successfully record three examples of neural activity in the isolated ventral nerve cord from three different preparations using three different NMTJs.

To drive the NMTJ with extracted signal from the crayfish, we utilized the experimental configuration shown in Fig. 1(c). We placed the NMTJ in a home-built probe station and connected to the input and output leads using a nonmagnetic picoprobe (10-50/30-125-BeCu-2-R-200, GGB Industries, Inc., Naples, FL, USA). An electromagnet applied a magnetic field along the in-plane minor axis of the device to produce precession of the magnetic free layer [Rowlands 2012]. We adjust the external magnetic field to the magnitude and direction that produced the highest power output. By applying the magnetic field, the free-layer magnetization is oriented along the in-plane minor axis of the device. We connected the silver electrodes from the crayfish neuron to the input port of the device. A bias tee separated out the direct electrical signal from the neuron from the induced microwave signal in the NMTJ. This technique provides access to both signals and enables us to compare the direct neuron activity to the device microwave response. We measured the electrical action potential from the lateral giant neuron using an oscilloscope (Lecroy HRO 64Zi). We measured the microwave signal using a low-noise amplifier (Pasternack PE15A1013) and a spectrum analyzer (Agilent 8564 EC). In order to improve the signal-to-noise ratio, we averaged the output microwave signal over 1000–6000 stimulation pulses at frequencies between 0.5–20 Hz.

III. RESULTS

We first characterized the NMTJ properties to determinate the strength of the external magnetic field that produced the maximum output. We drove the device with an external power supply and monitored the microwave response. Fig. 2 shows an average of 100 acquisitions of the power spectral density of the NMTJ output for different direct voltages as well as the measurements for the optimal external magnetic field of 10 mT that produced the maximum microwave

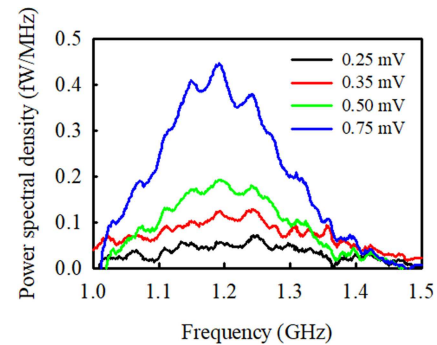


Fig. 2. Power spectral density of the microwave signal measured from the NMTJ for different input direct voltages with an in-plane magnetic field of 10 mT along the minor axis. Power curves show power measurements after normalizing for the amplifier gain.

power output. These measurements show the device oscillates with a frequency of 1.2 GHz, a bandwidth of 200 MHz, and with amplitudes ranging from 0.05 to 0.42 fW/MHz for the given voltages from 0.25 to 0.75 mV. From the measured resistance of the device ($600\ \Omega$), the voltage range corresponds to a peak input current in the range of 0.4 to $1.25\ \mu\text{A}$. Based on these currents, we conclude that the device works in the subthreshold regime where the applied current is below the critical current for zero-temperature onset of self-oscillations. In this case, the observed microwave signal arises from temperature-induced precession of magnetization of the free layer [Petit 2008]. In prior work, we were able to observe thermal oscillations with input currents as low as $300\ \mu\text{A}$, corresponding to a 300 mV driving voltage [Ramaswamy 2016]. Here, we found that by aligning the magnetic field along the minor axis of the NMTJ, instead of aligning out-of-plane as was done in Ramaswamy [2016], and by averaging over multiple acquisitions to reduce the noise, resulted in detectable signal levels when driving the NMTJ with voltages as low as 0.2 mV.

In order to drive the NMTJ with a current from an action potential, we applied repeated electrical stimuli to the lateral giant neuron to evoke action potentials, as explained in Section II. Fig. 3(a) shows the direct electrical signal from a crayfish neuron that we extracted from the inductive port of the bias tee. The black trace shows the voltage that we measured with the oscilloscope at the recording electrodes. In this specific case, the stimulus was a square pulse with an amplitude of 10 V and a duration of 0.2 ms. The initial spike (before 0.5 ms) in the voltage trace is the stimulus artifact due to direct coupling of the electrical signal from the stimulus electrode to the recording electrode. At approximately 1 ms after the stimulus, we observe a second voltage pulse that corresponds to an action potential, which reaches a maximum amplitude of 0.23 mV.

We next drove the NMTJ device directly with the output voltage of the neuron. The red trace in Fig. 3(a) shows the microwave power versus time at the frequency of 1.2 GHz with a bandwidth of 2 MHz (the maximum allowed bandwidth of the spectrum analyzer). To increase the signal-to-noise ratio, we recorded an average of 3000 sweeps (i.e., 3000 stimulations of the neuron). The instantaneous microwave output power follows the voltage waveform of the action potential (black trace). The large peaks at the beginning are due to direct activation of the NMTJ by the stimulus artifact. Following the stimulus artifact, we recorded another peak power 1 ms later, which matches the action potential. We found that the peak power that coincides with the action potential had a magnitude of 0.08 fW. We obtained similar re-

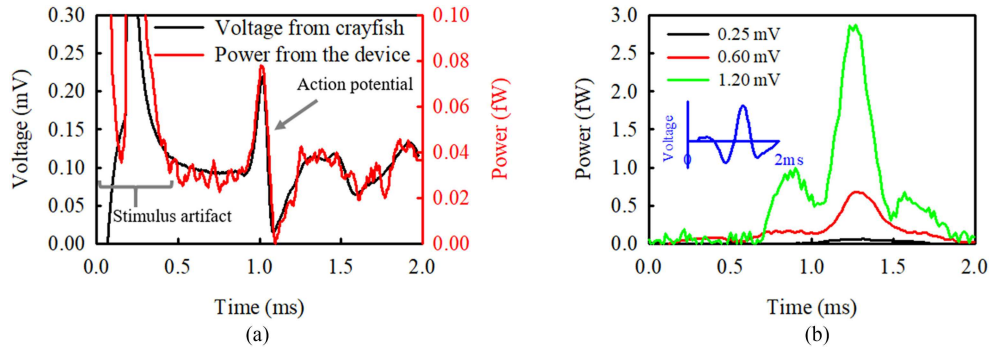


Fig. 3. (a) Action potential recorded from crayfish neurons using silver electrodes (black) and the corresponding microwave power measured from the NMTJ (red). (b) Microwave power from the NMTJ when excited with an artificial action potential (inset blue curve) of different amplitudes. Power curves show power measurements after normalizing for the amplifier gain.

sults at three different preparations using NMTJs working at different frequencies.

To determine the sensitivity of the device and assess the strength of the input signal, we generated artificial action potentials using an analog voltage waveform generator. We stimulated the NMTJ with input voltage pulses with temporal waveforms identical to those produced by a crayfish neuron (see Fig. 3(b) inset blue line). The waveforms we generated were based on recordings from a separate run on a crayfish neuron with no NMTJ. Because we performed extracellular recordings that measure the voltage difference between two electrodes placed on the crayfish neuron, the shape of the recorded signal depends on factors, such as the relative differences in distance between the two electrodes. For this reason, the simulated waveform has a different shape than the waveform recorded in Fig. 3(a). We artificially generated the action potential with the data acquisition board and the LabVIEW software and inputted it directly to the NMTJ by the inductive port of the bias tee. We employed action potentials with amplitudes of 0.25, 0.6, and 1.2 mV. Fig. 3(b) shows the microwave power output from the NMTJ versus time for artificial action potentials with a peak voltage range from 0.25 to 1.2 mV at a frequency of 1.2 GHz, with a bandwidth of 2 MHz. To discriminate the signal from the noise, we needed to average 1000 acquisitions for 0.25 mV action potential, 100 acquisitions for 0.6 mV, and 10 acquisitions for 1.2 mV. We observed peak power of 0.1, 0.8, and 2.8 fW for action potential amplitudes of 0.25, 0.6, and 1.2 mV, respectively. The power that we obtained for 0.25 mV with the artificial action potential agrees well with the result shown in Fig. 3(a). This result shows that increasing the peak voltage by 4.8 times produced a 28-fold increase in the peak power making the detection easier. Taking into account the device resistance (600Ω) input currents on the order of microamperes could provide single action potential detection.

IV. DISCUSSION

In summary, we demonstrated that action potentials from crayfish isolated nerve cords can generate microwave signals in NMTJs. The NMTJ device produced a peak power of 0.08 fW, which required averaging 3000 action potentials from a single neuron. The number of repetitions could be reduced by using a broader detection bandwidth similar to the signal bandwidth. The bandwidth in the current experiment is limited by the maximum spectrum analyzer bandwidth 2 MHz. By increasing the bandwidth up to the signal bandwidth 200 MHz, we could increase the signal about 20 dB, which is in the range of single-

shot detection. In prior work [Ramaswamy 2016], we showed that wireless detection entailed an additional 30 dB of loss in signal, which would render current signal levels undetectable. Various approaches can enhance the signal to overcome this additional loss and enable wireless detection. First, better antenna designs could significantly reduce the coupling loss, thereby increasing the signal. Furthermore, Fig. 3(b) shows that increasing the input current by a factor of 4.8 results in a 14 dB increase in signal. This current enhancement could be achieved by using NMTJs with lower resistance, which could produce larger currents for the same extracellular voltage levels. Devices with large-amplitude magnetization precession [Rowlands 2012, Maehara 2013] could further improve the sensing by emitting more power in a narrower bandwidth.

Ultimately, our results open up a new approach for high-resolution sensing of bioelectric signals using spintronic devices. NMTJs occupy a small device surface area, potentially in the nanoscale, and operate at low input currents, opening up the possibility for extremely dense low-power wireless sensor arrays. Furthermore, the oscillation frequency of these devices is highly tunable through the external magnetic field [Kiselev 2003, Slavin 2009]. In the presence of a strong magnetic field gradient, this property could enable NMTJs to encode their position in the oscillation frequency in an analogous way to magnetic resonance imaging. Furthermore, the small size of these devices opens up the possibility to introduce them intravenously. Previous studies showed that magnetic particles of similar dimensions can cross the blood-brain barrier and reach targets in the brain without disrupting the barrier in rat models [Kong 2012, Sensenig 2012]. One important consideration in such applications is the biocompatibility of magnetic devices. Previous work has demonstrated that proper polymer coating of magnetic devices enables them to be introduced into the body of a living organism without detrimental effects to neuronal activations [Jain 2008, Xiao 2011, Reddy 2012, Ramaswamy 2015, Wu 2015]. In addition to neuronal sensing, spintronic sensors could be useful for detecting electrical signals from other tissue such as heart, or other muscles. These properties could significantly enhance and extend current biological sensing capabilities.

ACKNOWLEDGMENT

This work was supported in part by a seed grant from the Brain and Behavior Initiative at the University of Maryland, College Park, MD, USA and in part by a National Science Foundation (NSF) BRAIN EAGER under Grant DBI1450921 as part of the BRAIN initiative. The work of Y.-J. Chen and I. N. Krivorotov on sample design and characterization was supported in part by the NSF under Grant DMR-1610146, Grant EFMA-1641989, and Grant ECCS-1708885; in part by the Army Research Office under

Grant W911NF-16-1-0472; and in part by the Defense Threat Reduction Agency under Grant HDTRA1-16-1-0025. The author thanks J. Langer and B. Ocker of Singulus Technologies for magnetic multilayer deposition, Dr. J. Rodger and B. Adissie for providing access to the microwave equipment, and P. V. del Rio who provided comments on this letter. The authors declare no competing financial interest.

REFERENCES

- Abdo A, Sahin M (2007), "NIR light penetration depth in the rat peripheral nerve and brain cortex," in *Proc. 29th Annu. Int. Conf. IEEE Eng. Med. Biol. Soc.*, vol. 2007, pp. 1723–1725, doi: [10.1109/IEMBS.2007.4352642](https://doi.org/10.1109/IEMBS.2007.4352642).
- Aston-Jones G, Deisseroth K (2013), "Recent advances in optogenetics and pharmacogenetics," *Brain Res.*, vol. 1511, pp. 1–5, doi: [10.1016/j.brainres.2013.01.026](https://doi.org/10.1016/j.brainres.2013.01.026).
- Belliveau J W, Kwong K K, Kennedy D N, Baker J R, Stern C E, Benson R, Chesler D A, Weisskoff R M, Cohen M S, Tootell R B H, Fox P T, Brady T J, Rosen B R (1992), "Magnetic resonance imaging mapping of brain function human visual cortex," *Investigative Radiol.*, vol. 27, pp. S59–S65, doi: [10.1097/00004424-199212002-00011](https://doi.org/10.1097/00004424-199212002-00011).
- Ben-Ari Y, Khalilov I, Kahle K T, Cherubini E (2012), "The GABA excitatory/inhibitory shift in brain maturation and neurological disorders," *Neuroscientist*, vol. 18, pp. 467–486, doi: [10.1177/1073858412438697](https://doi.org/10.1177/1073858412438697).
- Caruso L, Wunderle T, Lewis C M, Valadeiro J, Trauchessec V, Rosillo J T, Amaral J P, Ni J, Jendritza P, Fermon C, Cardoso S, Freitas P P, Fries P, Pannetier-Lecoecur M (2017), "In vivo magnetic recording of neuronal activity," *Neuron*, vol. 95, pp. 1283–1291, doi: [10.1016/j.neuron.2017.08.012](https://doi.org/10.1016/j.neuron.2017.08.012).
- Dale A M, Sereno M I (1993), "Improved localization of cortical activity by combining EEG and MEG with MRI cortical surface reconstruction: A linear approach," *J. Cogn. Neurosci.*, vol. 5, pp. 162–176, doi: [10.1162/jocn.1993.5.2.162](https://doi.org/10.1162/jocn.1993.5.2.162).
- Deac A M, Fukushima A, Kubota H, Maehara H, Suzuki Y, Yuasa S, Nagamine Y, Tsunekawa K, Djayaprawira D D, Watanabe N (2008), "Bias-driven high-power microwave emission from MgO-based tunnel magnetoresistance devices," *Nature Phys.*, vol. 4, pp. 803–809, doi: [10.1038/nphys1036](https://doi.org/10.1038/nphys1036).
- Edwards D H, Heitler W J, Krasne F B (1999), "Fifty years of a command neuron: The neurobiology of escape behavior in the crayfish," *Trends Neurosci.*, vol. 22, pp. 153–161, doi: [10.1016/S0166-2236\(98\)01340-X](https://doi.org/10.1016/S0166-2236(98)01340-X).
- Fenno L, Yizhar O, Deisseroth K (2011), "The development and application of optogenetics," *Annu. Rev. Neurosci.*, vol. 34, pp. 389–412, doi: [10.1146/annurev-neuro-061010-113817](https://doi.org/10.1146/annurev-neuro-061010-113817).
- Frahm J, Merboldt K-D, Hänicke W (1993), "Functional MRI of human brain activation at high spatial resolution," *Magn. Reson. Med.*, vol. 29, pp. 139–144, doi: [10.1002/mrm.1910290126](https://doi.org/10.1002/mrm.1910290126).
- Gerstner W, Kistler W M (2002), *Spiking Neuron Models: Single Neurons, Populations, Plasticity*. Cambridge, U.K.: Cambridge Univ. Press.
- Hämäläinen M, Hari R, Ilmoniemi R J, Knuutila J, Lounasmaa O V (1993), "Magnetoencephalography—Theory, instrumentation, and applications to noninvasive studies of the working human brain," *Rev. Mod. Phys.*, vol. 65, pp. 413–498, doi: [10.1103/RevModPhys.65.413](https://doi.org/10.1103/RevModPhys.65.413).
- Herberholz J, Marquart G D (2012), "Decision making and behavioral choice during predator avoidance," *Frontiers Neurosci.*, vol. 6, 125, doi: [10.3389/fnins.2012.00125](https://doi.org/10.3389/fnins.2012.00125).
- Herberholz J, Antonsen B L, Edwards D H (2002), "A lateral excitatory network in the escape circuit of crayfish," *J. Neurosci.*, vol. 22, pp. 9078–9085, doi: [10.1523/JNEUROSCI.22-20-09078.2002](https://doi.org/10.1523/JNEUROSCI.22-20-09078.2002).
- Herberholz J, Issa F A, Edwards D H (2001), "Patterns of neural circuit activation and behavior during dominance hierarchy formation in freely behaving crayfish," *J. Neurosci.*, vol. 21, pp. 2759–2767, doi: [10.1523/JNEUROSCI.21-08-02759.2001](https://doi.org/10.1523/JNEUROSCI.21-08-02759.2001).
- Herberholz J, Sen M M, Edwards D H (2004), "Escape behavior and escape circuit activation in juvenile crayfish during prey–predator interactions," *J. Exp. Biol.*, vol. 207, pp. 1855–1863, doi: [10.1242/jeb.00992](https://doi.org/10.1242/jeb.00992).
- Houssameddine D, Florez S H, Katine J A, Michel J-P, Ebels U, Mauri D, Ozatay O, Delaet B, Viala B, Folks L, Terris B D, Cyrille M-C (2008), "Spin transfer induced coherent microwave emission with large power from nanoscale MgO tunnel junctions," *Appl. Phys. Lett.*, vol. 93, 022505, doi: [10.1063/1.2956418](https://doi.org/10.1063/1.2956418).
- Jain T K, Reddy M K, Morales M A, Leslie-Pelecky D L, Labhasetwar V (2008), "Biodistribution, clearance, and biocompatibility of iron oxide magnetic nanoparticles in rats," *Mol. Pharmaceutics*, vol. 5, pp. 316–327, doi: [10.1021/mp7001285](https://doi.org/10.1021/mp7001285).
- Kiselev S I, Sankey J C, Krivorotov I N, Emley N C, Schoelkopf R J, Buhrman R A, Ralph D C (2003), "Microwave oscillations of a nanomagnet driven by a spin-polarized current," *Nature*, vol. 425, pp. 380–383, doi: [10.1038/nature01967](https://doi.org/10.1038/nature01967).
- Koch C, Segev I (2000), "The role of single neurons in information processing," *Nature Neurosci.*, vol. 3, pp. 1171–1177, doi: [10.1038/81444](https://doi.org/10.1038/81444).
- Kong S D, Lee J, Ramachandran S, Eliceiri B P, Shubayev V I, Lal R, Jin S (2012), "Magnetic targeting of nanoparticles across the intact blood–brain barrier," *J. Controlled Release*, vol. 164, pp. 49–57, doi: [10.1016/j.jconrel.2012.09.021](https://doi.org/10.1016/j.jconrel.2012.09.021).
- Maehara H, Kubota H, Suzuki Y, Seki T, Nishimura K, Nagamine Y, Tsunekawa K, Fukushima A, Deac A M, Ando K (2013), "Large emission power over 2 μW with high Q factor obtained from nanocontact magnetic-tunnel-junction-based spin torque oscillator," *Appl. Phys. Exp.*, vol. 6, 113005, doi: [10.7567/APEX.6.113005](https://doi.org/10.7567/APEX.6.113005).
- Mantegazza M, Curia G, Biagini G, Ragsdale D S, Avoli M (2010), "Voltage-gated sodium channels as therapeutic targets in epilepsy and other neurological disorders," *Lancet Neurol.*, vol. 9, pp. 413–424, doi: [10.1016/S1474-4422\(10\)70059-4](https://doi.org/10.1016/S1474-4422(10)70059-4).
- Mareschal D (2007), *Neuroconstructivism: How the Brain Constructs Cognition*. New York, NY, USA: Oxford Univ. Press.
- Matthews P M, Jezzard P (2006), "Functional magnetic resonance imaging," in *Neuroscience for Neurologists*, London, U.K.: Imperial College Press, pp. 401–422, doi: [10.1142/9781860948961_0015](https://doi.org/10.1142/9781860948961_0015).
- Meisler M H, Kearney J A (2005), "Sodium channel mutations in epilepsy and other neurological disorders," *J. Clin. Investigation*, vol. 115, pp. 2010–2017, doi: [10.1172/JCI25466](https://doi.org/10.1172/JCI25466).
- Millard A C, Jin L, Wei M-D, Wuskell J P, Lewis A, Loew L M (2004), "Sensitivity of second harmonic generation from styryl dyes to transmembrane potential," *Biophys. J.*, vol. 86, pp. 1169–1176, doi: [10.1016/S0006-3495\(04\)74191-0](https://doi.org/10.1016/S0006-3495(04)74191-0).
- Petit S, de Mestier N, Baraduc C, Thirion C, Liu Y, Li M, Wang P, Dieny B (2008), "Influence of spin-transfer torque on thermally activated ferromagnetic resonance excitations in magnetic tunnel junctions," *Phys. Rev. B*, vol. 78, 184420, doi: [10.1103/PhysRevB.78.184420](https://doi.org/10.1103/PhysRevB.78.184420).
- Popovic M, Vogt K, Holthoff K, Konnerth A, Salzberg B M, Grinvald A, Antic S D, Canepari M, Zecevic D (2010), "Imaging submillisecond membrane potential changes from individual regions of single axons, dendrites and spines," in *Membrane Potential Imaging in the Nervous System*. M. Canepari and D. Zecevic, Eds. New York, NY, USA: Springer, pp. 25–41.
- Ramaswamy B, Kulkarni S D, Villar P S, Smith R S, Eberly C, Araneda R C, Depireux D A, Shapiro B (2015), "Movement of magnetic nanoparticles in brain tissue: Mechanisms and impact on normal neuronal function," *Nanomedicine, Nanotechnol., Biol., Med.*, vol. 11, pp. 1821–1829, doi: [10.1016/j.nano.2015.06.003](https://doi.org/10.1016/j.nano.2015.06.003).
- Ramaswamy B, Algarin J M, Weinberg I N, Chen Y-J, Krivorotov I N, Katine J A, Shapiro B, Waks E (2016), "Wireless current sensing by near field induction from a spin transfer torque nano-oscillator," *Appl. Phys. Lett.*, vol. 108, 242403, doi: [10.1063/1.4953621](https://doi.org/10.1063/1.4953621).
- Reddy L H, Arias J L, Nicolas J, Couvreur P (2012), "Magnetic nanoparticles: Design and characterization, toxicity and biocompatibility, pharmaceutical and biomedical applications," *Chem. Rev.*, vol. 112, pp. 5818–5878, doi: [10.1021/cr300068p](https://doi.org/10.1021/cr300068p).
- Rippard W H, Pufall M R, Kaka S, Russek S E, Silva T J (2004), "Direct-current induced dynamics in Co₉₀Fe₁₀/Ni₈₀Fe₂₀ point contacts," *Phys. Rev. Lett.*, vol. 92, pp. 027201.1–027201.4, doi: [10.1103/PhysRevLett.92.027201](https://doi.org/10.1103/PhysRevLett.92.027201).
- Rothschild R M (2010), "Neuroengineering tools/applications for bidirectional interfaces, brain–computer interfaces, and neuroprosthetic implants—A review of recent progress," *Front Neuroeng.*, vol. 3, 112, doi: [10.3389/fneng.2010.00112](https://doi.org/10.3389/fneng.2010.00112).
- Rowlands G E, Krivorotov I N (2012), "Magnetization dynamics in a dual free-layer spin-torque nano-oscillator," *Phys. Rev. B*, vol. 86, 094425, doi: [10.1103/PhysRevB.86.094425](https://doi.org/10.1103/PhysRevB.86.094425).
- Sensenig R, Sapir Y, MacDonald C, Cohen S, Polyak B (2012), "Magnetic nanoparticle-based approaches to locally target therapy and enhance tissue regeneration in vivo," *Nanomedicine*, vol. 7, pp. 1425–1442, doi: [10.2217/nmm.12.109](https://doi.org/10.2217/nmm.12.109).
- Seo D, Neely R M, Shen K, Singhal U, Alon E, Rabaey J M, Carmena J M, Mahrbiz M M (2016), "Wireless recording in the peripheral nervous system with ultrasonic neural dust," *Neuron*, vol. 91, pp. 529–539, doi: [10.1016/j.neuron.2016.06.034](https://doi.org/10.1016/j.neuron.2016.06.034).
- Slavin A, Tiberkevich V (2009), "Nonlinear auto-oscillator theory of microwave generation by spin-polarized current," *IEEE Trans. Magn.*, vol. 45, pp. 1875–1918, doi: [10.1109/TMAG.2009.935](https://doi.org/10.1109/TMAG.2009.935).
- Swierzbinski M E, Lazarchik A R, Herberholz J (2017), "Prior social experience affects the behavioral and neural responses to acute alcohol in juvenile crayfish," *J. Exp. Biol.*, vol. 220, pp. 1516–1523, doi: [10.1242/jeb.154419](https://doi.org/10.1242/jeb.154419).
- Torrejon J, Riu M, Araujo F A, Tsunegi S, Khalsa G, Querlioz D, Bortolotti P, Cros V, Yakushiji K, Fukushima A, Kubota H, Yuasa S, Stiles M D, Grollier J (2017), "Neuromorphic computing with nanoscale spintronic oscillators," *Nature*, vol. 547, pp. 428–431, doi: [10.1038/nature23011](https://doi.org/10.1038/nature23011).
- Wine J J, Krasne F B (1983), "The cellular organization of crayfish escape behavior," in *The Biology of Crustacea*. Vol. 4, *Neural Integration and Behavior*, New York, NY, USA: Academic, vol. 4, pp. 241–292.
- Wu W, Wu Z, Yu T, Jiang C, Kim W-S (2015), "Recent progress on magnetic iron oxide nanoparticles: Synthesis, surface functional strategies and biomedical applications," *Sci. Technol. Adv. Mater.*, vol. 16, 023501, doi: [10.1088/1468-6996/16/2/023501](https://doi.org/10.1088/1468-6996/16/2/023501).
- Xiao L, Li J, Brougham D F, Fox E K, Feliu N, Bushmelev A, Schmidt A, Mertens N, Kiessling F, Valldor M, Fadeel B, Mathur S (2011), "Water-soluble superparamagnetic magnetite nanoparticles with biocompatible coating for enhanced magnetic resonance imaging," *ACS Nano*, vol. 5, pp. 6315–6324, doi: [10.1021/nn201348s](https://doi.org/10.1021/nn201348s).
- Zhang L, Fang B, Cai J, Carpentieri M, Puliafito V, Garescì F, Amiri P K, Finocchio G, Zeng Z (2018), "Ultrahigh detection sensitivity exceeding 10⁵ V/W in spin-torque diode," *Appl. Phys. Lett.*, vol. 113, 102401, doi: [10.1063/1.5047547](https://doi.org/10.1063/1.5047547).
- Zhou Y, Zha C L, Bonetti S, Persson J, Åkerman J (2008), "Spin-torque oscillator with tilted fixed layer magnetization," *Appl. Phys. Lett.*, vol. 92, 262508, doi: [10.1063/1.2955831](https://doi.org/10.1063/1.2955831).